

Table of contents

S1. Supplementary material and methods	1
S1.1. BRCT mutation panel design.....	1
S1.2. BRCT mutation panel construction.....	1
S1.3. BRCT screen: two-hybrid assay.....	2
S1.4. BRCT screen: NHEJ assays.....	2
S2. Supplementary Tables	4
Table S1. Yeast strains used in this study.....	4
Table S2. Dnl4 BRCT screening panel.....	5
Table S3. Fusion primers used to generate mutations.....	8
S3. Supplementary figures	11
Figure S1. Dnl4 BRCT screening panel.....	11
Figure S2. BRCT screen methods.....	14
Figure S3. BRCT screen results.....	15
Figure S4. Correlation between precise and imprecise NHEJ.....	15
Figure S5. Structural representation of Dnl4 BRCT mutations.....	16
Figure S6. Yeast two-hybrid assay control plates.....	16
Figure S7. Imprecise joints in the suicide deletion assay.....	18
S4. Supplementary references	19

S1. Supplementary material and methods

S1.1. BRCT mutation panel design

Primary sequence alignments of the Dnl4 BRCT region across various species were made using ClustalW (1), MACAW (2) and manual editing to judge positions which were invariant or where residue properties such as charge or hydrophobicity were conserved (Figure S1A). Structural alignments of human (3) and yeast (4) crystal structures (Figure S1B), in which the tandem LIG4/Dnl4 BRCT domains were bound to the coiled-coil domain of XRCC4/Lif1, were taken as supplied by NCBI VAST (5) and visualized using Cn3D (6). Mutant Dnl4 BRCT constructs (Figure S1, Table S2) were designed to encompass as many conserved residues as possible in a panel that would fit into a single 96-well plate, which was achieved by combining some mutations into compound double point mutations.

S1.2. BRCT mutation panel construction

To screen a large number of Dnl4 BRCT domain mutations, we adopted a gap repair strategy (Figure S2) similar to the one previously used to create two-hybrid constructs (7). Two separate BRCT region PCR products were made for each target mutation that overlapped at their internal

ends that bore the new mutation as part of the corresponding PCR primers (see Table S3 for sequences). These two PCR products were co-transformed into yeast with a *Sma*I-linearized plasmid such that the overlap between the PCR products drove three-way gap repair and reconstituted a complete mutated BRCT domain in the plasmid. The low efficiency of blunt plasmid recircularization by NHEJ and high efficiency of gap repair led to very high fragment incorporation rates in transformants. PCR products were not purified from template DNA prior to gap repair in order to avoid excessive handling. Thus, the pool of transformants contained low levels of gap repair resulting from wild-type BRCT template DNA, estimated to be approximately 1%. PCR reactions, transformations and most downstream steps were handled in 96-well plates with the assistance of a robotic pipettor. At the end of transformation by the LiAc protocol (8,9), bulk yeast in LiAc/PEG solution were diluted 100-fold into liquid selective medium and allowed to recover for two days prior to further handling.

S1.3. BRCT screen: two-hybrid assay

For determination of Lif1 interaction, BRCT region gap repair was performed using yeast strain YW740 and the two-hybrid bait plasmid pOBD2 (10). The transformant pool was recovered in -Trp medium and mated in bulk to yeast strain YW624 bearing the two-hybrid bait prey pOAD-Lif1(137-265) (7). Following limiting dilution spotting, three individual diploid colonies for each mutant were picked, expanded, and plated to -Leu-Trp control plates and -His and -Ade two-hybrid indicator plates. After 3 days, Dnl4(651-944)–Lif1(137-265) interaction was scored on a scale from 0 (no detectable interaction) to 3 (equivalent to wild-type). When only one of three colonies was scored as 3, that colony was inferred to be a likely wild-type contaminant and the screen score was determined from the remaining clones.

S1.4. BRCT screen: NHEJ assays

For determination of NHEJ efficiency, the gap repair target plasmid, pTW671, contained the native *DNL4* promoter and coding sequence corresponding to amino acids 1 to 681 and the *HDF1* terminator in the *LEU2*-selected pTW435 backbone (7), such that gap repair with the mutated BRCT region PCR products restored full-length *DNL4*. The yeast strain, YW1657, was a *dnl4*Δ derivative of YW1276, which bears the previously described HO(+1) suicide deletion assay (7,11). In this assay, precise NHEJ yields a frame-shifted *ADE2* reporter gene and Ade⁻/red yeast, while imprecise NHEJ by the high frequency +CA imprecise joint restores the *ADE2* reading frame and yields Ade⁺/white yeast. Precise NHEJ was scored by plating the expanded transformant pools, without cloning, to parallel glucose -Leu and galactose -Leu plates and

scoring fractional survival on galactose (“exp” in Figure S3) relative to glucose (“ctl”). Imprecise NHEJ as a fraction of all *ADE2* locus repair was scored by diluting the expanded transformant pools 100-fold into liquid galactose -Leu medium to allow DSB induction and repair to occur, followed by plating to parallel glucose -Leu and glucose -Leu-Ade plates and scoring fractional survival on -Leu-Ade (“exp”) relative to -Leu (“ctl”). Final results were expressed as a percentage of wild-type NHEJ determined from the silent mutations.

S2. Supplementary Tables

Table S1. Yeast strains used in this study

Strain	Genotype
YW1657	<i>MATα ade2::HOSD(+1)::STE3-MET15 dnl4Δ::URA3 his3Δ1 leu2Δ0 lys2Δ0 met15Δ0 ura3Δ0</i>
YW1228	<i>MATα ade2::SD2::STE3-MET15 his3Δ1 leu2Δ0 met15Δ0 ura3Δ0</i>
YW1230	YW1228 <i>dnl4Δ::KanMX4</i>
YW2045	YW1228 <i>dnl4-D800K</i>
YW2047	YW1228 <i>dnl4-GG(868:869)AA</i>
YW2048	YW1228 <i>dnl4-KTT(742:744)ATA</i>
YW2051	YW1228 <i>dnl4-L750*</i>
YW2052	YW1228 <i>dnl4-F836*</i>
YW2053	YW1228 <i>dnl4-D796*</i>
YW2218	YW1228 <i>dnl4-D800K, dnl4-GG(868:869)AA</i>
YW2299	YW1228 <i>dnl4-K742A</i>
YW2300	YW1228 <i>dnl4-T744A</i>
YW2083	<i>MATα ade2-M7 his3Δ200 leu2- lys2-801 trp1Δ63 ura3-52</i>
YW1993	<i>MATα-inc::AmpR-35S can1Δ::Gal1HO-QPCR DNL4-13Myc::HisMX6 GAL 1prm -HOcs gal1::HO his3Δ1 leu2Δ0 met15Δ0 ura3Δ0</i>
YW2036	YW1993 <i>dnl4-D800K-13Myc::HisMX6</i>
YW2038	YW1993 <i>dnl4-GG(868:869)AA-13Myc::HisMX6</i>
YW2039	YW1993 <i>dnl4-KTT(742:744)ATA-13Myc::HisMX6</i>
YW2219	YW1993 <i>dnl4-D800K, GG(868:869)AA -13Myc::HisMX6</i>
YW2301	YW1993 <i>dnl4-K742A-13Myc::HisMX6</i>
YW2302	YW1993 <i>dnl4-T744A-13Myc::HisMX6</i>
YW2121	YW1993 <i>lif1Δ::KanMX4</i>
YW2122	YW1993 <i>nej1Δ::KanMX4</i>
YW2166	<i>MATα-inc::AmpR-35S can1Δ::GAL 1-QPCR LIF1-13Myc::hisMX6 GAL 1prm-HOcs gal1::HO his3Δ1 leu2Δ0 met15Δ0 ura3Δ0</i>
YW2167	YW2166 <i>dnl4Δ::kanMX4</i>
YW2214	YW2166 <i>dnl4-D800K</i>
YW2215	YW2166 <i>dnl4-GG(868:869)AA</i>
YW2216	YW2166 <i>dnl4-KTT(742:744)ATA</i>
YW2217	YW2166 <i>dnl4-L750*</i>

Table S2. Dnl4 BRCT screening panel

For each screening mutation or control construct (Figure S1), NHEJ values are tabulated as the average across two replicates while the two-hybrid result is the composite call after considering all replicates (see Figure S3 and Supplementary Materials and Methods). Two-hybrid scores range from 0 (no detectable interaction) to 3 (equivalent to wild-type). Mutations are sorted by position except for the controls in the top six rows.

Mutation	Precise NHEJ (%WT)	Imprecise NHEJ (%WT)	Two-hybrid Score
L750L (=wt)	89.5	112.5	3
S813S (=wt)	113	110	3
Q875Q (=wt)	95.5	76.5	3
L750*	15.5	0	0
A789*	19	2	0
F836*	89.5	31	1
F686A	107	72.5	0
G688A	101.5	88	2
L689A	99	79	3
SD(695:696)AA	43	67	1
Y697A	102	63.5	3
TG(702:703)AA	72.5	114	3
RIT(705:707)AIA	105	102	3
I706A	155	141	3
RAE(708:710)AAA	120.5	102.5	3
E712A	142.5	113.5	3
IV(715:716)AA	129.5	81	1
GG(719:720)AA	94.5	64	0
GK(720:721)AA	115	96.5	1
LI(722:723)AA	98.5	45	3
N725A	114	59	3
L728A	74.5	83	3
K729A	209.5	96.5	3
R737A	144.5	89	1
SC(740:741)AA	124	117	3
K742E	35.5	36.5	3
KTT(742:744)ATA	8.5	0	2
EC(746:747)AA	42	56	3
CK(747:748)AA	116.5	85	3
LI(750:751)AA	13	0	3
DR(752:753)AA	106	101	3
R753E	61.5	42	3

Mutation	Precise NHEJ (%WT)	Imprecise NHEJ (%WT)	Two-hybrid Score
GYD(754:756)AYA	169.5	115	0
Y755A	59	97	3
D756K	105.5	47.5	0
HP(759:760)AA	90	27	2
W762A	136.5	94	0
D765K	106	137	3
DC(765:766)AA	85	105	1
Y769A	109.5	74	3
K770A	98	69	3
L772A	114.5	97	3
I775A	89.5	80.5	3
E776K	84	99	0
EP(776:777)AA	88	100.5	0
YCF(779:781)ACA	97	101.5	0
CFN(780:782)AFA	86.5	100	3
FNV(781:783)ANA	134.5	108.5	0
NVS(782:784)AVA	109.5	111.5	3
EK(792:793)AA	89.5	88.5	3
RVD(794:796)AVA	34.5	21	0
V795A	143.5	98	3
D796K	91	48.5	0
GD(799:800)AA	73.5	50.5	0
D800K	61	46	0
SFE(801:803)AFA	74	87	1
F802A	93.5	81.5	0
I806A	113.5	96	3
SE(807:808)AA	125	73	3
L811A	149.5	87	2
S812A	143.5	73	3
SQ(817:818)AA	149	99	3
D830K	135	78	2
DSE(830:832)ASA	85.5	116.5	2
P837A	102	65.5	1
LF(838:839)AA	135.5	100	0
LF(840:841)AA	52.5	16	0
R844A	74	61.5	1
IAY(845:847)AAA	65	76	0
P849A	130.5	70.5	2
KIK(863:865)AIA	67	78.5	0
IKL(864:866)AKA	103	98	0
LF(866:867)AA	81.5	56	0
GG(868:869)AA	51	85	0

Mutation	Precise NHEJ (%WT)	Imprecise NHEJ (%WT)	Two-hybrid Score
KIT(870:872)AIA	103	73	1
L877A	116.5	71.5	3
CN(878:879)AA	108	60.5	0
P884A	104	76.5	1
P888A	59	117	2
KD(892:893)AA	85	92.5	3
PK(913:914)AA	99	67	3
I915A	74.5	118.5	3
R917A	70	41.5	3
PE(921:922)AA	105	68	3
WV(923:924)AA	53	12.5	0
DHS(925:927)AHA	88	74.5	0
I928A	106.5	70	0
NCQ(931:933)ACA	92.5	78	1
V934A	46	49	3
PE(935:936)AA	67	115.5	1
EED(936:938)KRK	60	36	0
ED(937:938)AA	47.5	61.5	3
DFP(938:940)AFA	82.5	85.5	3
FPV(939:941)APA	69	88	0

Table S3. Fusion primers used to generate mutations

Fusion primers are the internal primers that bore the mutations in Figure S2

Mutation	Forward	Reverse
L750L (=wt)	TGCAAGGCTCTCATAGATCGAGGATATGATATATTG	CGATCTATGAGAGCCTTGCAATCCGTGGTAG
S813S (=wt)	CAAACGTGCATCCTTGATATAAATCACAACCTAAGTCTA	ATTTATACAAGGATGACAGTTTGGTTTCCGAAATG
Q875Q (=wt)	AACAGATCAACAATCACTTTGTAACCTAATAATTATAC	TACAAAGTGATTGTTGATCTGTTATTTTCCACCAA
L750*	TGCAAGGCTTGAATAGATCGAGGATATGATATATTG	TCGATCTATTCAAGCCTTGCAATCCGTGGTAG
A789*	AAAAATGAGATGAGTCGCTGAAAAAGGGTAGAT	TTCAGCGACTCATCTCATTTTTTTGAGAGACGTAA
F836*	GTTTCGGCGGTGACCATTATTTTTATTCTCCAACAG	AATAATGGTCACCGCCGAACCTCAGAATCT
F686A	TCAAACATCGCAGCCGATTACTTTTTTATGTTC	AATCCGGCTGCGATGTTTGAATTTGGCAGTTGT
G688A	CATCTTTGCCGATTACTTTTTTATGTTCTCTCTGAC	AAAAAGTAATGCGGCAAAGATGTTTGAATTTGGC
L689A	CTTTGCCGAGCACTTTTTTATGTTCTCTCTGACTA	ATAAAAAAGTGCTCCGGCAAAGATGTTTGAATTT
SD(695:696)AA	ATGTTCTCGCAGCATATGTCACGGAGGACACTGG	TGACATATGCTGCGAGAACATAAAAAAGTAATCCGG
Y697A	TCTCTGACGCAGTCACGGAGGACACTGGAA	TCCGTGACTGCGTCAGAGAGAACATAAAAAAGTA
TG(702:703)AA	GGAGGACGCAGCAATACGGATTACACGGGCAGA	CCGTATTGCTGCGTCTCCGTGACATAGTCAG
RIT(705:707)AIA	GAATAGCAATCGCACGGCAGAACTTGAAAAAAGT	GCCCGTGCGATTGCTATTCCAGTGCTCTCCGTGA
I706A	GAATACGGGCAACACGGGCAGAACTTGAAAAA	GCCCGTGTTGCCGTATTCCAGTGCTCTCC
RAE(708:710)AAA	ATTACAGCAGCAGCACTTGAAAAAAGTATTGTGGAACA	TTCAAGTGCTGCTGCTGTAATCCGTATTCCAGTGTC
E712A	GGCAGAACTTGCAAAAAGTATTGTGGAACATGGTG	AATAGTTTTTGCAAGTTCTGCCCGTGAATCC
IV(715:716)AA	GAAAAAAGTGCAGCAGAACATGGTGGTAAACTGATAT	CATGTTCTGCTGCAGTTTTTTCAAGTTCTGCCCG
GG(719:720)AA	TGGAACATGCAGCAAAAGTATATAATGTAATTTTAAAA	TCAGTTTTGCTGCATGTTCCACAATAGTTTTTTCAAG
GK(720:721)AA	AACATGGTGCAGCACTGATATATAATGTAATTTTAAAAACG	ATATCAGTGCTGCACCATGTTCCACAATAGTTTTTT
LI(722:723)AA	GGTGGTAAAGCAGCATATAATGTAATTTTAAAACGTCATTC	CATTATATGCTGCTTTACCACCATGTTCCACAATA
N725A	AACTGATATATGCAGTAATTTTAAAACGTCATTCAATTG	TTTTAAAATTACTGCATATATCAGTTTACCACCATGTT
L728A	ATAATGTAATTGCAAAACGTCATTCAATTGGGGAC	AATGACGTTTTGCAATTACATTATATATCAGTTTACCA
K729A	TGTAATTTTAGCACGTCATTCAATTGGGGACGT	TTGAATGACGTGCTAAAATTACATTATATATCAGTTTAC
R737A	GGGGACGTTGCATTAATCAGCTGTAAAAGTACCAC	CTGATTAATGCAACGTCACCAATGAAATGACG
SC(740:741)AA	CGGTTAATCGCAGCAAAAGTACCACGGAATGCAAG	TAGTTTTTGCTGCGATTAACCGAACGTCACCAA
K742E	ATCAGCTGTGAGACTACCACGGAATGCAAGGC	GTGGTAGTCTCAGCTGATTAACCGAACGTC
KTT(742:744)ATA	GCTGTGCAACCGCAACGGAATGCAAGGCTTTAATAG	CCGTTGCGGTTGCACAGCTGATTAACCGAACGTC
EC(746:747)AA	TACCACGGCAGCAAAAGGCTTTAATAGATCGAGGAT	AGCCTTTGCTGCCGTGGTAGTTTTACAGCTGAT
CK(747:748)AA	CCACGGAAGCAGCAGCTTTAATAGATCGAGGATATG	TAAAGCTGCTGCTCCGTGGTAGTTTTACAGCT
LI(750:751)AA	CAAGGCTGCAGCAGATCGAGGATATGATATATTGC	TCGATCTGCTGCAGCCTTGCAATCCGTGGTAG
DR(752:753)AA	GCTTTAATAGCAGCAGGATATGATATATTGCACCCAA	CATATCCTGCTGCTATTAAAGCCTTGCAATCCGTG
R753E	CTTTAATAGATGAGGGATATGATATATTGCACCCAA	TATCATATCCCTCATCTATTAAAGCCTTGCAATCC
GYD(754:756)AYA	GATCGAGCATAACGAATATTGCACCCAAATGGGTAC	CAATATTGCGTATGCTCGATCTATTAAAGCCTTGCAAT
Y755A	GATCGAGGAGCAGATATATTGCACCCAAATGGG	CAATATATCTGCTCCTCGATCTATTAAAGCCTTG
D756K	TCGAGGATATAAGATATTGCACCCAAATGGGTAC	GTGCAATATCTTATATCCTCGATCTATTAAAGCC
HP(759:760)AA	GATATATTGGCAGCAAAATGGGTACTCGATTGTATAG	CCCAATTTGCTGCCAATATATCATATCCTCGATCTA
W762A	CACCCAAATGCAGTACTCGATTGTATAGCATATAA	TCGAGTACTGCATTTGGGTGCAATATATCATATC
D765K	TGGGTACTCAAGTGTATAGCATATAAGAGGCTCA	TGCTATACACTGAGTACCAATTTGGGTGCA

Mutation	Forward	Reverse
DC(765:766)AA	GGGTACTCGCAGCAATAGCATATAAGAGGCTCATCC	TGCTATTGCTGCGAGTACCCAATTTGGGTGCA
Y769A	TGTATAGCAGCAAAGAGGCTCATCCTGATCGA	GAGCCTCTTTGCTGCTATAACAATCGAGTACCCA
K770A	ATAGCATATGCAAGGCTCATCCTGATCGAGC	GATGAGCCTTGCCATATGCTATAACAATCGAGTACC
L772A	TATAAGAGGGCAATCCTGATCGAGCCCAATTAT	GATCAGGATTGCCCTCTTATATGCTATAACAATCG
I775A	TCATCCTGGCAGAGCCCAATTATTGCTTTAACG	TTGGGCTCTGCCAGGATGAGCCTCTTATATGC
E776K	CATCCTGATCAAGCCCAATTATTGCTTTAACGTCT	ATAATTGGGCTTGATCAGGATGAGCCTCTTATA
EP(776:777)AA	ATCCTGATCGCAGCAAAATTATTGCTTTAACGTCTCTCA	AATAATTTGCTGCGATCAGGATGAGCCTCTTATA
YCF(779:781)ACA	CCCAATGCATGCGCAAACGTCTCTCAAAAAATGAGAG	ACGTTTGCGCATGCATTGGGCTCGATCAGGATGA
CFN(780:782)AFA	CAATTATGCATTCGCAGTCTCTCAAAAAATGAGAGCC	AGAGACTGCGAATGCATAATTGGGCTCGATCAGGAT
FNV(781:783)ANA	TATTGCGCAAACGCATCTCAAAAAATGAGAGCCGTC	TTGAGATGCGTTTGCGCAATAATTGGGCTCGATCAG
NVS(782:784)AVA	TGCTTTGCAGTCGCACAAAAAATGAGAGCCGTCGC	TTTTTGTGCGACTGCAAAGCAATAATTGGGCTCGATC
EK(792:793)AA	CGTCGCTGCAGCAAGGGTAGATTGTTGGGTGAT	ACCCTTGCTGCAGCGACGGCTCTCATTTTTTTG
RVD(794:796)AVA	GAAAAAGCAGTCGCATGTTTGGGTGATAGTTTTGAAA	CAAACATGCGACTGCTTTTTTCAGCGACGGCTCTCA
V795A	TGAAAAAGGGCAGATTGTTTGGGTGATAGTTTTG	CAAACAATCTGCCCTTTTTTCAGCGACGGCTC
D796K	AAAAAGGGTAAAGTGTTTGGGTGATAGTTTTGAAA	ACCCAAACACTTTACCCTTTTTTCAGCGACGG
GD(799:800)AA	GATTGTTTGGCAGCAAGTTTTGAAAATGACATTTCCGGA	CAAACCTTGCTGCCAAACAATCTACCCTTTTTTCAG
D800K	TTGTTTGGGTAAGAGTTTTGAAAATGACATTTCCGGA	TTTCAAAACTCTTACCCAAACAATCTACCCTTTTT
SFE(801:803)AFA	GGTGATGCATTCGCAAATGACATTTCCGAAACCAAAC	GTCATTTGCGAATGCATCACCCAAACAATCTACCCT
F802A	GGTGATAGTGCAGAAAATGACATTTCCGAAACCA	GTCATTTTCTGCACTATCACCCAAACAATCTACC
I806A	GAAAATGACGCATCGGAAACCAAACGTGCATCA	GGTTTCCGATGCGTCATTTTTCAAACACTATCACCC
SE(807:808)AA	ATGACATTCAGCAACCAAACACTGTATCATTTGTATAA	GTTTGGTTGCTGCAATGTCATTTTTCAAACACTATCACCC
L811A	GGAAACCAAAGCATCATCATTTGTATAAAATCACAACATA	CAATGATGATGCTTTGGTTTTCCGAAATGTCATTTT
S812A	AACCAAACACTGGCATCATTTGTATAAAATCACAACATAAGT	ATACAATGATGCCAGTTTGGTTTTCCGAAATGTC
SQ(817:818)AA	TTGTATAAAGCAGCACTAAGTCTACCACCGATGGG	GACTTAGTGCTGCTTTATAACAATGATGACAGTTTGG
D830K	CTCGAGATAAAGTCTGAGGTTCCGGCGGTTTC	AACCTCAGACTTTATCTCGAGTTCCCCCATCG
DSE(830:832)ASA	GAGATAGCATCCGCAGTTCGGCGGTTTCCATTATTT	CGAACTGCGGATGCTATCTCGAGTTCCCCCATCG
P837A	TCGGCGGTTTGCATTATTTTTATTCTCCAACAGGAT	TAAAAATAATGCAAACCGCCGAACCTCAGAAT
LF(838:839)AA	GGTTTTCCAGCAGCATTATTCTCCAACAGGATTGCAT	AGAATAATGCTGCTGGAAACCGCCGAACCTCA
LF(840:841)AA	CCATTATTTGCAGCATCCAACAGGATGCATACGTA	TGTTGGATGCTGCAAATAATGGAAACCGCCGAAC
R844A	TTCTCCAACGCAATTGCATACGTACCACGTCG	GTATGCAATTGCGTTGGAGAATAAAAAATAATGGAAA
IAY(845:847)AAA	ACAGGGCAGCAGCAGTACCACGTCGAAAATTAGC	GGTACTGCTGCTGCCCTGTTGGAGAATAAAAAATAATG
P849A	GCATACGTAGCAGTCGCAAAATTAGCACAGAA	TTGCGACGTGCTACGTATGCAATCCTGTTGGA
KIK(863:865)AIA	AGAAATGGCAATCGCATTGTTTGGTGAAAAATAACAGA	AAACAATGCGATTGCCATTTCTATAATGTCATCTCTG
IKL(864:866)AKA	AATGAAAGCAAAGGCATTTGGTGAAAAATAACAGATCA	ACCAAATGCCTTTGCTTTTCAATTTCTATAATGTCATCTTC
LF(866:867)AA	AAATTAAGGCAGCAGGTTGAAAAATAACAGATCAAC	TTCCACCTGCTGCCTTAATTTTCATTTCTATAATGTCAT
GG(868:869)AA	AAGTTGTTTGCAGCAAAAAATAACAGATCAACAGTCACT	GTTATTTTTGCTGCAAACAACCTTAATTTTCATTTCTATAA
KIT(870:872)AIA	GGTGGAGCAATCGCAGATCAACAGTCACTTTGTAAC	TGATCTGCGATTGCTCCACCAAACAACCTTAATTTTCA
L877A	TCAACAGTCAGCATGTAACCTAATAATTATACCATATAC	TAAGTTACATGCTGACTGTTGATCTGTTATTTTTTC
CN(878:879)AA	CAGTCACTTGCGCATTAATAATTATACCATATACTGATC	TTATTAATGCTGCAAGTACTGTTGATCTGTTATTT
P884A	TAATAATTATAGCATATACTGATCCTATTTTGGAGAA	GGATCAGTATATGCTATAATTATTAAGTTACAAAGTGAC
P888A	ATATACTGATGCAATTTTGGAGAAAGACTGCATGA	TCCTCAAAATGTCATCAGTATATGGTATAATTATTAAG
KD(892:893)AA	TTTTGAGGGCAGCATGCATGAATGAGGTACACGAA	CATGCATGCTGCCCTCAAAATAGGATCAGTATATG

Mutation	Forward	Reverse
PK(913:914)AA	GATACTATAGCAGCAATAGCCAGGGTCGTTGCC	TGGCTATTGCTGCTATAGTATCAGAAGCCTTTATTTG
I915A	TACCGAAAGCAGCCAGGGTCGTTGCCCT	ACCTGGCTGCTTTCGGTATAGTATCAGAAGCC
R917A	AAAATAGCCGCAGTCGTTGCCCTGAATGGG	GCAACGACTGCGGCTATTTTCGGTATAGTATCA
PE(921:922)AA	CGTTGCCGCAGCATGGGTGGATCATTCTATTAATG	ACCCATGCTGCGGCAACGACCCTGGCTATT
WV(923:924)AA	CCCCTGAAGCAGCAGATCATTCTATTAATGAAAAGTGT	ATGATCTGCTGCTTCAGGGGCAACGACCCTG
DHS(925:927)AHA	TGGGTGGCACACGCAATTAATGAAAAGTGTCAAGTGCC	TTAATTGCGTGTGCCACCCATTCAGGGGCAACG
I928A	GGATCATTCTGCAAATGAAAAGTGTCAAGTGCCCTG	GTTTTCATTTGCAGAATGATCCACCCATTCAGG
NCQ(931:933)ACA	ATGAAGCATGCGCAGTGCCCTGAAGAAGACTTCCC	GGCACTGCGCATGCTTCATTAATAGAATGATCCACCC
V934A	AACTGTCAAGCACCTGAAGAAGACTTCCCCG	TTCTTCAGGTGCTTGACAGTTTTTCATTAATAGAATG
PE(935:936)AA	GTCAAGTGGCAGCAGAAGACTTCCCCGTAGTCAA	GTCTTCTGCTGCCACTTGACAGTTTTTCATTAATAG
EED(936:938)KRK	GTGCTAAGCGAAAGTCCCCGTAGTCAACTACTG	GGGAAGTTTCGCTTAGGCACCTTGACAGTTTTTCATTA
ED(937:938)AA	GCCTGAAGCAGCATTCCCCGTAGTCAACTACTG	GGGAATGCTGCTTCAGGCACCTTGACAGTTTTTC
DFP(938:940)AFA	GAAGAAGCATTTCGAGTAGTCAACTACTGATGGTGC	GACTACTGCGAATGCTTCTTCAGGCACCTTGACAGTT
FPV(939:941)APA	GAAGACGCACCAGCAGTCAACTACTGATGGTGCCT	GTTGACTGCTGGTGCCTTCTTCAGGCACCTTGACA

S3. Supplementary figures

Figure S1. Dnl4 BRCT screening panel

The residues affected by the mutations in Table S2 are depicted in two formats.

(A) Multiple sequence alignment of the Dnl4 BRCT region against selected yeasts. Mammalian species are not included due to the substantial primary sequence divergence in the region. Sc, *S. cerevisiae*; Sp, *S. paradoxus*; Sm, *S. mikatae*; Scas, *S. castellii*; Ag, *Ashbya gossypii*; Ca, *Candida albicans*. Red shading, identical among all displayed proteins; black shading, identical to Sc Dnl4; grey shading, conserved relative to Sc Dnl4.

(B) The same *S. cerevisiae* Dnl4 region (yDnl4) compared to human LIG4 (hLIG4), where sequences have been aligned by secondary and tertiary structure (3,4). Uppercase residues are those judged by VAST (5) to be in structural alignment. Secondary structural elements detected by Cn3D (6) are: orange, beta sheet; green, alpha helix. One conserved primary sequence motif surrounding mutation D800K is indicated: “[”, identical; “.” conserved.

In (A) and (B), blue circles mark the position of an introduced stop codon and triangles mark residues altered in at least one construct, with red triangles highlighting mutations KTT(742:744)ATA, D800K, and GG(868:869)AA studied in further detail.

< figures next pages >

Figure S1B

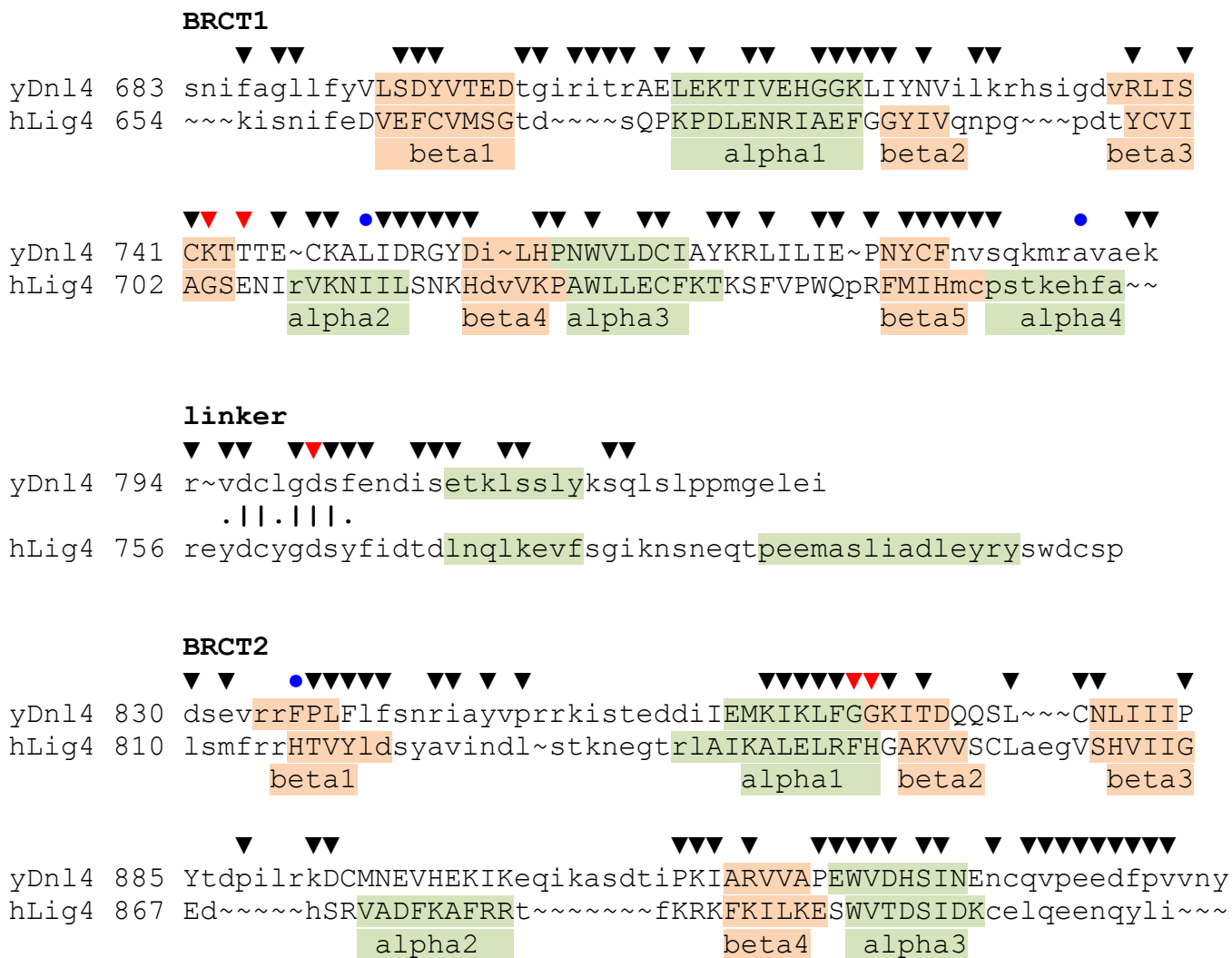


Figure S2. BRCT screen methods

Diagram of the PCR and gap repair strategy. An asterisk represents the target mutation being created, X figures represent recombination that occurs in the yeast to assemble the intact BRCT region. Different plasmids were used for the NHEJ and two-hybrid assays. Yeast transformation mixes were grown in bulk liquid cultures without cloning for precise and imprecise NHEJ assays prior to plating as indicated. Diploid clones were obtained for two-hybrid constructs following mating to a Lif1 indicator strain and plated for scoring as indicated. A diagram of the HOSD(+1) suicide deletion NHEJ assay has been provided previously (7) (it is similar to the I-SceI assay in Figure 5A). Its key properties are that two galactose-induced HO-mediated DSBs are created in the chromosomal *ADE2* locus in a manner such that precise NHEJ yields *Ade⁻*/red yeast capable of growing on galactose plates while +2 imprecise NHEJ yields *Ade⁺*/white yeast capable of growing in the absence of adenine.

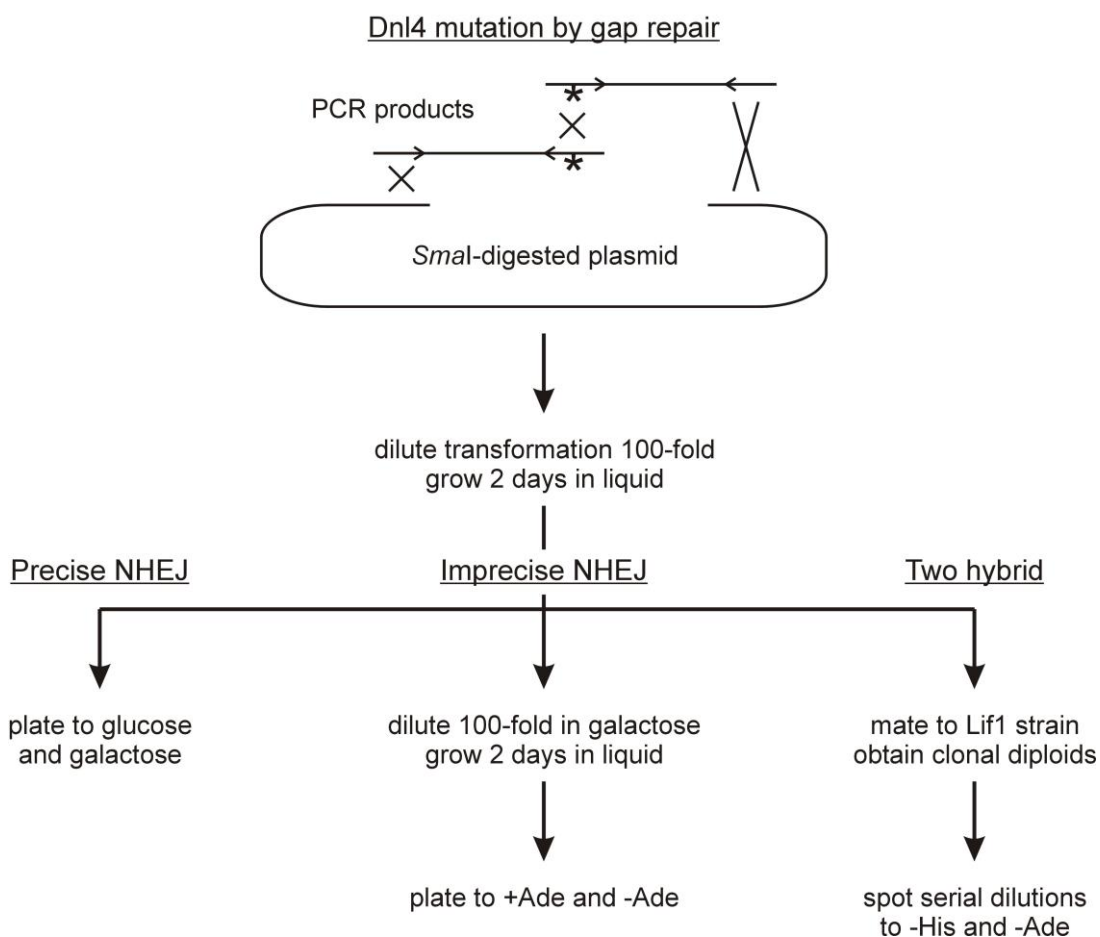


Figure S3. BRCT screen results

The accompanying PDF file (Figure_S3.pdf) contains one data panel for each screened mutation. Rows within a panel correspond to replicates (Rep1, etc.), with two replicates for the NHEJ measurements and three replicates for the two-hybrid measurements. Columns show colony counts for experimental (“exp”) and control (“ctl”) plates and final results expressed as % of wild-type for the precise and imprecise HOSD(+1) NHEJ assays. Increased intensity of red shading in the %wt columns provides a visual cue to samples with increased degrees of NHEJ defect. Cropped and assembled two-hybrid spot images, at two 10-fold dilutions, reveal the degree of Lif1 interaction as growth on -His and -Ade indicator plates. Occasional clonal wild-type contaminants are observed for the two-hybrid assay. The first block shows results for a control in which no primers were added to the PCR reaction, to demonstrate that the background of the screening approach was wild-type Dnl4.

< see file Figure_S3.pdf >

Figure S4. Correlation between precise and imprecise NHEJ

Panel showing a correlation plot and linear regression line of precise to imprecise NHEJ in the screen. Each point represents a single mutant.

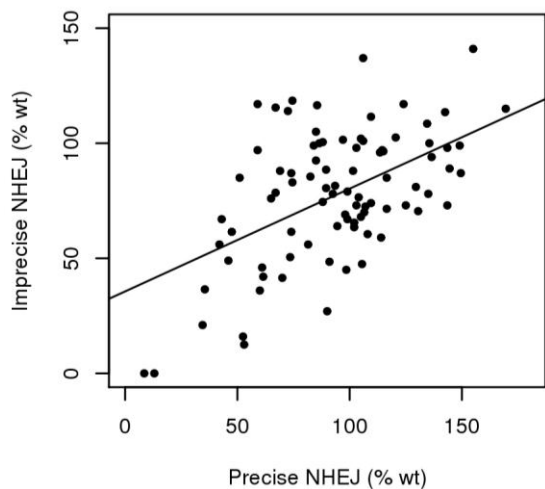


Figure S5. Structural representation of Dnl4 BRCT mutations

(A) The Dnl4–Lif1 interaction interface from PDB 1Z56 [6]. The Lif1 coiled-coil (grey) and Dnl4 BRCT region (green) are depicted in ribbon diagram. The mutated Dnl4-D800 (red) and GG(868-9) (magenta) residues, as well as two Lif1 lysine residues (blue) within 5 Å of Dnl4-D800, are shown in stick form.

(B) Identical to (A) except in surface representation. Residues Dnl4-D800 and Lif1-KK(219-20) are still shaded red and blue, respectively, but are completely buried within the protein interface and not visible. The tight packing of Dnl4-G868 against the Lif1 coiled-coil is barely visible. A strongly disruptive influence on Dnl4-Lif1 interaction is thus predicted for Dnl4 D800K and GG(868:869)AA mutations.

(C) Similar to (A), zoomed out to show the entire Dnl4 BRCT region. Side chains of residues K742 and T744, altered in mutation KTT(742:744)ATA and highlighted in red, are solvent exposed and distant from the Dnl4-Lif1 interaction interface.

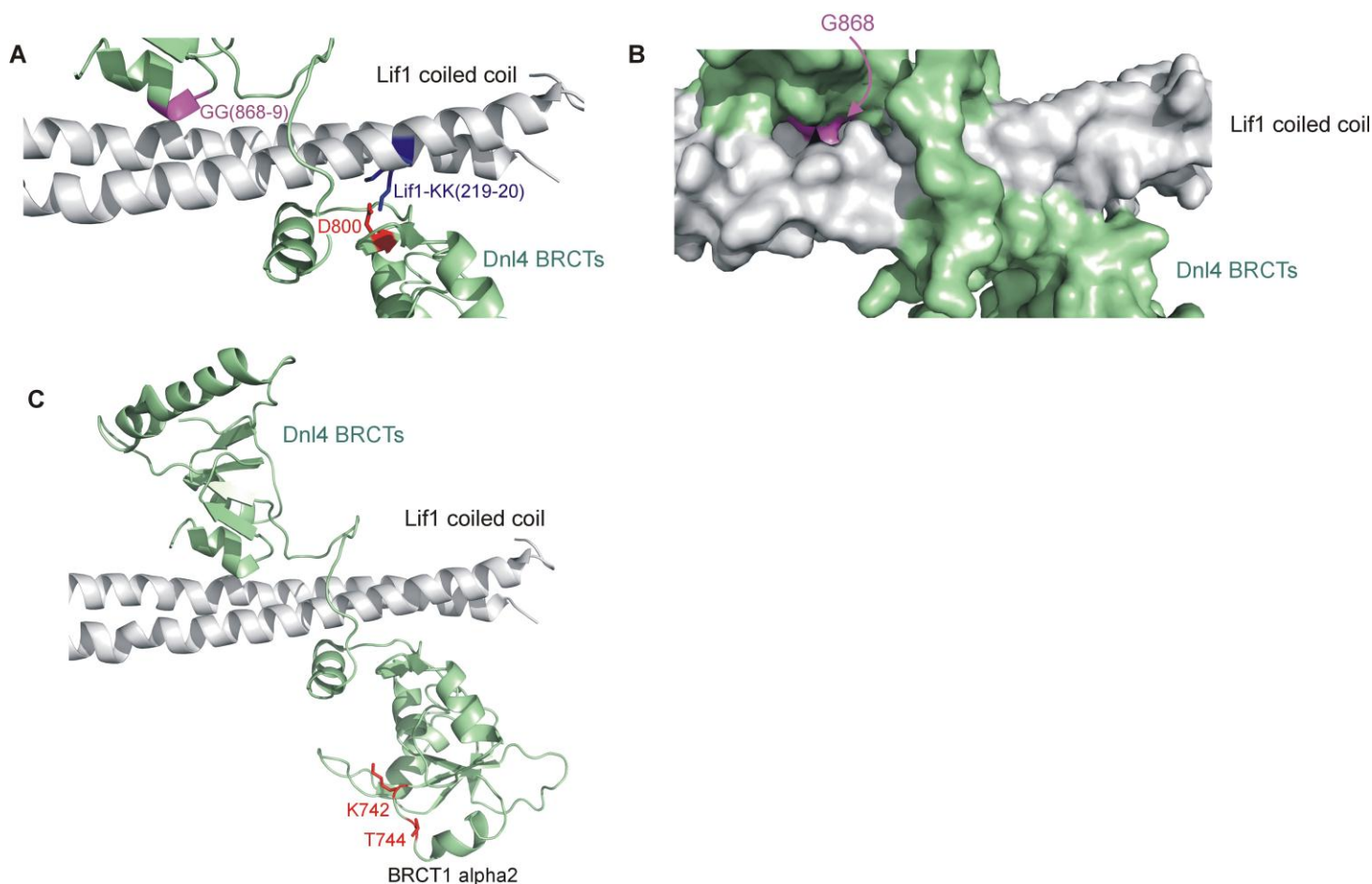


Figure S6. Yeast two-hybrid assay control plates

(A) to (C) Panels showing the –Leu –Trp control plates for the strains from Figure 2 to demonstrate the equivalent growth of the strains without selection. Because of the *ADE2* reporter allele in the strains, a productive Dnl4-Lif1 interaction can be observed as a white colony appearance.

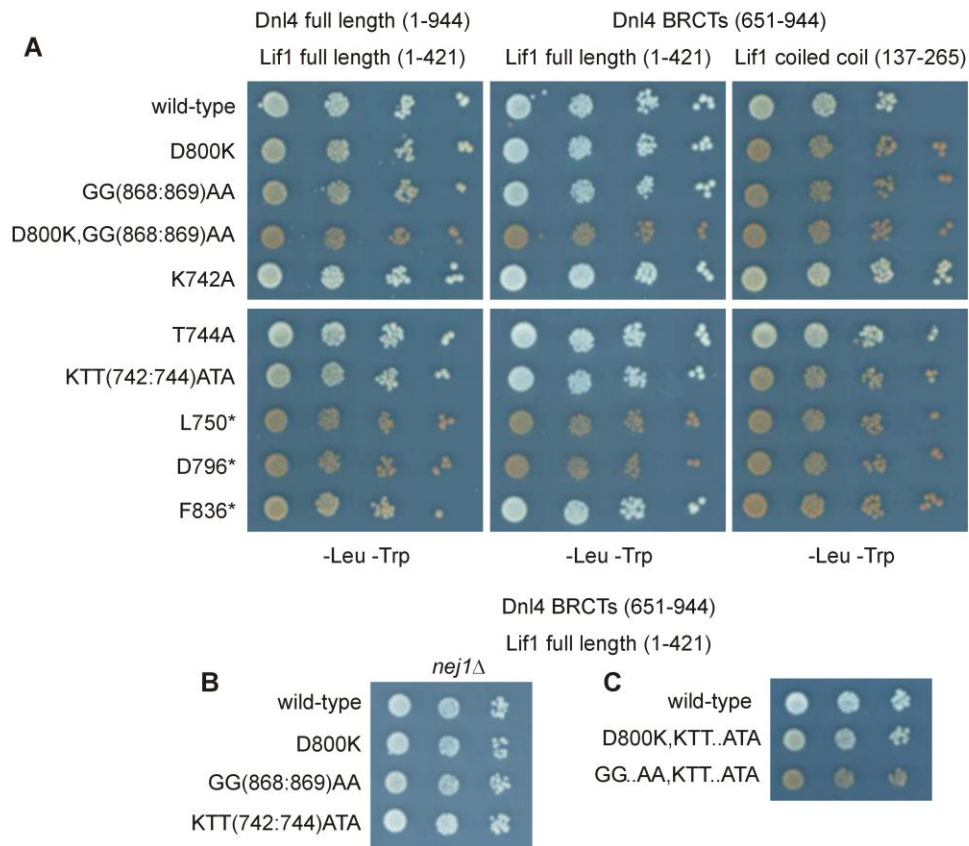


Figure S7. Imprecise joints in the suicide deletion assay

The sequence at the top left shows the product of precise suicide-deletion NHEJ, equivalent to an I-SceI cut site. Bold type shows the location of the 4-base 3' overhang. Subsequent lines show imprecise joints and the number of times they were observed in Dnl4 mutant strains.

Underlined bases are microhomologies, dashes indicate deleted bases, and lower case indicates inserted bases that cannot be accounted for by the DSB substrate.

GATAAACGCGTGTATTACCCTG TTAT CCCTAGCGTCAGATCCTCTAGAA	Wild-type	D800K	GG(868:869)AA
GATAAACGCGTGTATTA----- <u>CCCT</u> -----AGCGTCAGATCCTCTAGAA	6/10	4/10	4/10
GATAAAC----- <u>GCGT</u> -----CAGATCCTCTAGAA	3/10	3/10	3/10
GATAAACGCGTGTATTACCCTG <u>TTA</u> -----GCGTCAGATCCTCTAGAA	1/10		
GATAAACGCGTGTA----- <u>TAT</u> CCCTAGCGTCAGATCCTCTAGAA		1/10	
GATAAACGCGTGTATTA----- <u>C</u> -----GTCAGATCCTCTAGAA			1/10
GA----- <u>TA</u> -----GAA			1/10
GATAAA-----AGCGTCAGATCCTCTAGAA		1/10	
GATAAACGCGTGTATTACCCTG-----GCGTCAGATCCTCTAGAA			1/10
GATAAACGCGTGTATTACCCTGTTATt atCCCTAGCGTCAGATCCTCTAGAA		1/10	

S4. Supplementary references

1. Chenna, R., Sugawara, H., Koike, T., Lopez, R., Gibson, T.J., Higgins, D.G. and Thompson, J.D. (2003) Multiple sequence alignment with the Clustal series of programs. *Nucleic Acids Res*, **31**, 3497-3500.
2. Schuler, G.D., Altschul, S.F. and Lipman, D.J. (1991) A workbench for multiple alignment construction and analysis. *Proteins*, **9**, 180-190.
3. Wu, P.Y., Frit, P., Meesala, S., Dauvillier, S., Modesti, M., Andres, S.N., Huang, Y., Sekiguchi, J., Calsou, P., Salles, B. *et al.* (2009) Structural and functional interaction between the human DNA repair proteins DNA ligase IV and XRCC4. *Mol. Cell. Biol.*, **29**, 3163-3172.
4. Dore, A.S., Furnham, N., Davies, O.R., Sibanda, B.L., Chirgadze, D.Y., Jackson, S.P., Pellegrini, L. and Blundell, T.L. (2006) Structure of an Xrcc4-DNA ligase IV yeast ortholog complex reveals a novel BRCT interaction mode. *DNA Repair*, **5**, 362-368.
5. Gibrat, J.F., Madej, T. and Bryant, S.H. (1996) Surprising similarities in structure comparison. *Curr. Opin. Struct. Biol.*, **6**, 377-385.
6. Wang, Y., Geer, L.Y., Chappey, C., Kans, J.A. and Bryant, S.H. (2000) Cn3D: sequence and structure views for Entrez. *Trends in Bioch. Sci.*, **25**, 300-302.
7. Palmbo, P.L., Daley, J.M. and Wilson, T.E. (2005) Mutations of the Yku80 C terminus and Xrs2 FHA domain specifically block yeast nonhomologous end joining. *Mol. Cell. Biol.*, **25**, 10782-10790.
8. Daley, J.M., Laan, R.L., Suresh, A. and Wilson, T.E. (2005) DNA joint dependence of pol X family polymerase action in nonhomologous end joining. *J. Biol. Chem.*, **280**, 29030-29037.
9. Daley, J.M. and Wilson, T.E. (2005) Rejoining of DNA double-strand breaks as a function of overhang length. *Mol. Cell. Biol.*, **25**, 896-906.
10. Uetz, P., Giot, L., Cagney, G., Mansfield, T.A., Judson, R.S., Knight, J.R., Lockshon, D., Narayan, V., Srinivasan, M., Pochart, P. *et al.* (2000) A comprehensive analysis of protein-protein interactions in *Saccharomyces cerevisiae*. *Nature*, **403**, 623-627.
11. Della, M., Palmbo, P.L., Tseng, H.M., Tonkin, L.M., Daley, J.M., Topper, L.M., Pitcher, R.S., Tomkinson, A.E., Wilson, T.E. and Doherty, A.J. (2004) Mycobacterial Ku and ligase proteins constitute a two-component NHEJ repair machine. *Science*, **306**, 683-685.